

Received March 29, 2021; reviewed; accepted April 22, 2021

## Application of EIS technique to investigate the adsorption of different types of depressants on pyrite

Zeliha Ertekin <sup>1</sup>, Kadir Pekmez <sup>1</sup>, Ronel Kappes <sup>2</sup>, Zafir Ekmekçi <sup>3</sup>

<sup>1</sup> Hacettepe University, Department of Chemistry, Beytepe, Ankara-06800, Turkey

<sup>2</sup> Newmont Corporation, 10101 E Dry Creek Road, Englewood CO 80112, USA

<sup>3</sup> Hacettepe University, Department of Mining Engineering, Beytepe, Ankara- 06800, Turkey

Corresponding author: zelihaertekin@hacettepe.edu.tr (Zeliha Ertekin)

**Abstract:** Batch scale flotation tests are generally performed for testing effects of flotation reagents on flotation performance. This method becomes costly and time-consuming for testing a number of flotation reagents such as collectors, depressants and activators. Therefore, developing alternative low-cost, fast and sensitive methods have recently been the subject of intense research to obtain a better flotation performance. The electrochemical techniques have been used for the surface characterization of sulfide minerals. Electrochemical Impedance Spectroscopy (EIS) is one of these techniques that can provide significant information related to surface characteristics, reagent adsorption on the sulfide minerals. In this study, EIS was used as an alternative technique to the conventional batch scale flotation tests for pre-screening of various flotation reagents using two pyrite samples containing different contents of Au and As. Sodium cyanide (NaCN), sodium metabisulfite (SMBS), and a polymeric depressant Aero 7261A were tested as depressants for two pyrite samples (Sample A from a Carlin-trend ore and Sample B from a Sulfidic ore from South America) having different electrochemical characteristics. EIS results showed that the effects of the sequence of addition of collector (Potassium amyl xanthate - KAX) and depressant were also investigated to evaluate the stability of depressant and collector compounds formed at the surface. The sequence of addition of the collector and depressants was significant for Sample A but not for Sample B. The results show that EIS can be used as an effective tool for testing the performance of various flotation reagents and their mixtures on sulfide minerals.

**Keywords:** pyrite, depressants, collector, mineral electrodes, electrochemical impedance spectroscopy

### 1. Introduction

Pyrite (FeS<sub>2</sub>, iron disulfide) is known as the earth's most abundant sulfide mineral. It is often associated as a gangue mineral with valuable sulfide minerals containing copper, lead, zinc, and gold (Li et al, 2016; Chandra and Gerson 2010; Moslemi and Gharaghi 2017; Rath et al. 2000). It is one of the most common sulfide minerals used in studying transition metal sulfides because of its excellent properties such as electrochemical performance, degradation, optical, and electronic properties (Lai et al, 2012).

Flotation is a physico-chemical separation process used as an industrial process for selectively separating valuable minerals from gangue (Ai et al, 2017). Iron sulfide minerals (pyrite, arsenian pyrite and arsenopyrite) are often considered as sulfide gangue minerals in many of these flotation processes, and the flotation chemistry is adjusted for the depression of these minerals. However, in some gold ores, these minerals, particularly arsenian pyrite, are considered valuable minerals as they contain gold, and hence the flotation chemistry is adjusted to increase their flotation kinetics and recovery (Kappes et al, 2010).

Many researchers have shown that there is a strong relationship between electrochemical reactions occurring on the pyrite surface and its flotation process (Moslemi and Gharaghi 2017). The presence of arsenic changes the electrochemical properties of arsenian pyrite and arsenopyrite, and increases rate

of surface oxidation. The selective separation of sulfide minerals by flotation mostly relies on the use of various collectors and depressants (Li et al. 2015). Collectors adsorb on the mineral surface, increase hydrophobicity to enhance attachment of air bubbles and flotation to the froth phase (Ackerman et al, 1987). Depressants are known as modifiers that influence the attachment of collectors to the mineral surface. Collectors for pyrite flotation include xanthate, dithiophosphate, dithiocarbamate, thionocarbamate, and thiourea, among which, xanthate is preferred mostly due to its strong collecting ability (Huang et al, 2019; Mu et al, 2020). Inorganic reagents containing sulfides, hydroxides, cyanide, and hydrogen peroxide are commonly used as depressants for pyrite flotation (Rath et al., 2000; Huang et al, 2019). Therefore, it is important to know the effects of depressants on surface chemistry and flotation behaviour of the sulfide minerals in flotation.

The flotation of sulfide minerals depends on the electrochemical reactions occurring on the mineral surface (Moslemi and Gharaghi 2017; Pauporte and Schuhmann 1996). Separation performance of flotation reagents and mechanism of selective separation were investigated through various laboratory scale flotation methods, contact angle measurements, surface analytical techniques such as X-ray Photoelectron Spectroscopy (XPS), Tof-SIMS, Raman Spectroscopy, etc. and electrochemical techniques (Zhang et al, 2019; Velasquez et al 2005; Valdivieso et al 2004; Zheng et al, 2019). The XPS technique is costly and involves complex data processing for analyzing the changes in oxidation state of diverse chemical elements on the surface of minerals. The simpler surface characterization techniques such as zeta potential and contact angle measurements are also used for surface chemistry studies. However, these techniques should be used with other surface analytical methods to understand the interactions and the type of species occurring on the surface. Therefore, many researchers prefer the electrochemical tools for surface characterization of the sulfide minerals as they are considered sensitive and reproducible analytical techniques with high accuracy, allowing an in-situ detection of the formation of surface layers on the mineral electrode (Guo et al, 2020). The most common electrochemical techniques used in the sulfide minerals research include cyclic voltammetry (CV), open circuit potential (OCP), polarization curves, electrochemical impedance spectroscopy (EIS), potentiometry, and coulometry, etc. (Mu et al, 2017). The EIS measurement technique is the most effective technique as it can be used to determine the species formed on mineral surfaces independent of the type of reactions (Zhao et al, 2017). EIS measurements pack multiple frequencies in a short duration signal, thus enabling its use in understanding both slow and fast reactions.

In recent years, the use of EIS has become a more generally applied technique by many authors to investigate the physical and chemical processes occurring at mineral/electrolyte interfaces (Mu et al, 2017; Nicol, 2017). Mu et. al. investigated the effect of three lignosulfonate-based biopolymers (DP-1775, DP-1777, and DP-1778) as pyrite depressants using EIS, and showed that DP-1778 was the strongest depressant for pyrite, followed by DP-1775 and DP-1777 (Mu et al, 2016a). Studies on the adsorption behavior of the pyrite-xanthate-cyanide system at pH 5 via CV and EIS were performed by Guo (Guo, 2016). This study reported that the pyrite surface upon xanthate adsorption was poisoned by cyanide with the formation of an iron cyanide complex (Prestidge et al, 1993).

Effects of various flotation reagents (collectors, activators, depressant) on flotation performance are generally determined by bench-scale flotation tests, which require a large amount of material, costly and time-consuming. However, it is very well known that most of the sulfide minerals are semiconductor with variable electrochemical properties, which mainly depends on ore genesis, surface defects and also the association with other sulfide minerals (Abramov and Avdohin, 1997). Therefore, electrochemical techniques are suitable for investigating surface chemistry, adsorption of flotation reagents, and thus determining floatability of the sulfide minerals under various flotation conditions. The electrochemical techniques require a small amount of materials compared to bench-scale flotation tests. A large number of parameters can be tested in a relatively short time and at a relatively low cost. For most of the sulfide minerals, a direct correlation between collector adsorption and electrochemical response could be observed (Allison et al., 1972; Goold and Finkelstein 1972; Ekmeçi et al, 2010). Therefore, it is possible to use an electrochemical measurement as a proxy to estimate the adsorption of flotation reagents (collectors, activators, depressants) and hence correlate with flotation behaviour.

Inorganic depressants (cyanide, hydroxyl ions, sulfur-oxy species, etc.) and organic depressants (polysaccharides polymers, lignosulfonate-based biopolymers, polyacrylamide polymers, etc) have been

widely used in mineral separation (Mu et al, 2016). Among these, cyanide is known as an effective depressant for pyrite flotation. The depression of pyrite flotation by cyanide may reduce the mixed potential and inhibit the electrochemical activity on the pyrite surface. Sulfur-oxy species such as metabisulfite ( $S_2O_5^{2-}$ ) have also been used in flotation as pyrite depressants to replace cyanide. The mechanism of pyrite depression by sulfoxyl species is rather complex, and it is indicated that the presence of sulfite consumes dissolved oxygen leading to a drop of the pulp potential. Moreover, copper sulfite precipitation maybe occurs that limit the extent of activation of pyrite. Organic depressants have attracted considerable attention as alternative depressants due to their rich sources, biodegradable nature and relatively low cost (Bicak et al, 2007). However, organic depressants such as polyacrylamide are thought to adsorb on the mineral surface via various interactions because they are complex polymer structures. Mineral depression using polymer depressants depends on their chemical characteristics such as functional groups, charge density and molecular weight, and a number of mechanisms can be proposed. For example, electrochemical attraction can be formed between oppositely charged polymer and mineral surfaces. Also, hydrophobic interaction can be achieved between non-polar segments of polymer chains and hydrophobic areas of mineral surfaces. Hydrogen bonds may form between hydroxyl groups and hydrated metallic sites on mineral surfaces, or chemical interactions between the anionic functional groups (such as carboxylate or sulfonic groups) and the metallic cations on mineral surfaces may cause the binding of polymers (Mu et al, 2016).

In a previous study, the authors used EIS as the prime electrochemical technique to investigate the adsorption mechanisms of different types of collectors on pyrite (Ertekin et. al, 2016). In this study, the adsorption behaviour of NaCN, sodium metabisulfite (SMBS), and Aero7261A (a polymeric depressant from Solvay) was investigated by the EIS technique in presence and absence of collector. Two pyrite samples having different chemical and mineralogical characteristics were used in the experiments. The impact of the sequence of addition of collector and depressant was also discussed. This study demonstrates that EIS technique can be used as a fast and low-cost reagent pre-screening technique in the flotation of sulfide ores.

## 2. Materials and methods

### 2.1. Materials

Two samples containing mainly pyrite, arsenopyrite, and arsenian pyrite as iron sulfide minerals and three different depressants were used. Sample A was prepared from a Carlin trend ore, and Sample B from a sulfidic ore from South America. Sample A was taken from the final pyrite concentrate of a gold-pyrite flotation process, and Sample B from the pyrite scavenger flotation concentrate of a different gold-pyrite flotation process. The mineral content of Sample A and Sample B was identified by XRD measurement. The results of the analysis were determined by Rietveld analysis of XRD patterns (Ertekin et. al, 2016). Mineralogical characterization showed that Sample B was composed of 70% pyrite, 19% quartz, and 11% pyrophyllite. Sample A was composed of 48% quartz, 27% pyrite, and 10% illite with lesser amounts of pyrite (2.38%) and arsenopyrite (1.44%). Chemical analysis of the two samples is given in Table 1. Sample A has high Au and As, but lower sulfide mineral content compared to Sample B.

Table 1. Chemical analysis of Sample A and Sample B

Pyrite samples	S %	Fe %	Al %	Au ppm	As ppm	Ag ppm	Cu ppm	Zn ppm	Ca ppm
Sample A	12.26	12.84	4.42	9.111	6527	6.3	612	4541	7644
Sample B	40.02	34.23	1.94	1.103	794	14.3	3204	107	207

In the literature, Carlin trend ores are described as being generally difficult to treat. These ores typically have to undergo several additional processing stages for gold recovery (Kappes and Gathje, 2010). Arsenian pyrite typically contains the majority of the gold values for Carlin-trend ores. Arsenic-bearing minerals are not very easy to separate from other valuable (non-arsenic-bearing) minerals, and they can be difficult to selectively depress with standard depressants (Kappes et al, 2010).

Sodium cyanide (NaCN, Aldrich > 97%), sodium metabisulphite (SMBS, Merck,  $\geq 99.5\%$ ), and Aero7261A (Solvay) were used as depressants in the experiments. Aero7261A is a modified polyacrylamide based water-soluble polymer recommended for depression of iron sulphide minerals. The functionalized polymer is a proprietary blend and developed as an alternative to cyanide as a depressant in flotation. Probably, various functional groups such as carboxyl, sulfonate, hydroxyl or thiourea attached to polyacrylamide polymer can depress iron sulfide minerals. The interaction between mineral surface and polymer depends on the type of reacting groups in their complex chemical structure. Technical grade potassium amyl xanthate (KAX) was used as a collector. All electrochemical experiments were performed in a buffer solution (pH 9.2) of 0.05 M  $\text{Na}_2\text{B}_4\text{O}_7 \cdot 10\text{H}_2\text{O}$  (Merck,  $\geq 99.5\%$ ). Depressant and collector concentrations were set to 200 ppm in all EIS measurements. This is a typical concentration used in most of the surface chemistry studies to obtain multilayer adsorption (Mu et al, 2016b). High purity nitrogen was used to provide an inert atmosphere for electrochemical measurements. All chemicals were purchased from commercial sources and were of the highest purity available. They were used without further purification.

## 2.2. Preparation of mineral electrodes and electrochemical measurements

The sulfide mineral content of a mineral electrode should be high to obtain a large surface area in the electrode for getting a better electrochemical response. Pyrite content of Sample B was 70% which was sufficient to fabricate the mineral electrode. However, Sample A contains only 27% iron sulfide minerals, which should be increased to get a strong electrochemical signal. Therefore, a dry electrostatic separation technique was applied to separate the non-sulfide minerals and increase the sulfide mineral content of the sample before electrode fabrication. The electrostatic separation method is a physical process and uses the differences in electrical conductivity of the minerals. Pyrite is a good conductor mineral, while quartz is an insulator (Knoll and Taylor, 1985). The electrostatic separation experiment increased the amount of sulfide minerals by 30% in Sample A, which was suitable for the use of mineral electrode fabrication.

A novel mineral electrode fabrication method was used to prepare the electrodes using two different pyrite samples, as described in the published papers of the authors (Ertekin et al, 2016; Ekmekçi et al, 2016). In this study, the samples were taken from flotation concentrates, and the sulfide mineral particles were expected to be covered with flotation reagents. Therefore, both samples were washed by diluted HCl and acetone sequentially. After that, the samples were rinsed with distilled water to remove any oxidized and organic species from the surface. The washed samples were dried in a vacuum desiccator and then homogenized with graphite and a conductive binder (conductive polymer polyaniline) to produce a pellet of 1.3 cm diameter. The mineral electrode was fabricated by mounting the pellet in an electrochemical inert epoxy resin. In the literature, electrode polishing is a well-known procedure. The alumina, silicon carbide, diamond, or boron carbide are commonly used for electrode polishing, depending on the applications (Monteiro and Koper, 2019). The most common procedure for graphite containing surface is polishing the prepared electrode with alumina paste (Kariuki, 2012). Before the electrochemical experiments, the electrode surface was polished using alumina paste to create a fresh surface, which allowed the use of the same electrode for all electrochemical experiments performed in this study.

The surface area of Sample A and Sample B mineral electrodes was measured by using an optical microscope equipped with Clemex Image Analysis system as 0.39  $\text{cm}^2$  and 0.43  $\text{cm}^2$  respectively (Fig. 1).

Various electrochemical methods can be employed for surface chemistry analysis of sulfide minerals. In this study, EIS was used to investigate the changes in surface characteristics of the pyrite particles in the mineral electrodes. Gamry Reference 600 Potentiostat-Galvanostat was used with a faraday cage. The measurements were performed in a standard three-electrode electrochemical cell containing a standard calomel electrode (reference electrode), a platinum wire (counter electrode), and a mineral electrode (working electrode). All EIS measurements were performed in the frequency range of  $1 \times 10^5$  to  $1 \times 10^{-2}$  Hz. All potentials shown in this paper were converted to the standard hydrogen electrode (SHE) scale. A constant polarization potential (100 mV) was applied during EIS measurements. The buffer solution (pH 9.2) of 0.05 M  $\text{Na}_2\text{B}_4\text{O}_7 \cdot 10\text{H}_2\text{O}$  was used as an electrolyte, and all measurements

were carried out at room temperature ( $\sim 25^\circ\text{C}$ ). The pyrite electrodes were polished with alumina and thoroughly rinsed before each experiment. High purity de-ionized water was used in all experiments.

The impedance spectrum can be modelled by an electrical circuit with physical elements to explain a simple charge transfer process at the mineral/solution interface (Zhao et al, 2017). In this study, the EIS data of pyrite electrodes in the absence and presence of depressants and collector (KAX), were fitted to an equivalent electrical circuit using Gamry Echem Analyst software. Various equivalent circuit models were examined to describe the processes on the electrode surface (pyrite/collector or depressant/electrolyte junction). The equivalent electrical circuit with the smallest chi-square ( $\chi^2$ ) value was chosen, as shown in Fig. 2. Thus, minimum errors were obtained. A similar equivalent circuit model was used to explain the electrochemical process on the pyrite electrode surface (Guo, 2016; Guo et al, 2016).

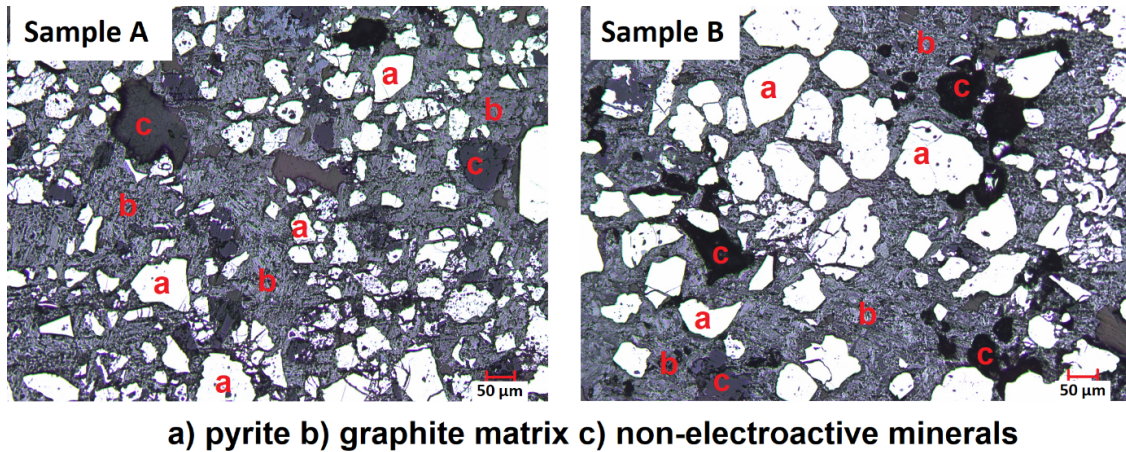


Fig. 1. Optical microscope image of polished mineral electrode surfaces of Sample A and Sample B

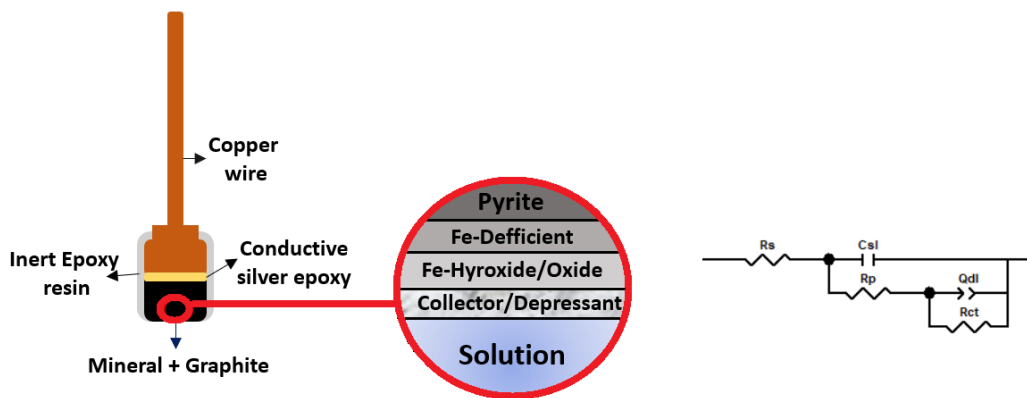


Fig. 2. Schematic view of the mineral electrode with an equivalent electrical circuit for modeling adsorption of depressants, collector, and the sequence of addition of collector and depressants

Pyrite is a natural semiconductor, and the electrochemical reactions on the electrode surface can take place easily according to electrooxidation of reaction on pyrite surface in alkaline media. Iron species such as  $\text{Fe}(\text{OH})_3$ ,  $\text{FeOOH}$ , and  $\text{FeSO}_4$  may form at the surface (Velasquez et. al, 2005; Jiang et al 1988). As shown in Fig. 2,  $R_s$  is the electrolyte resistance, and  $R_{ct}$  represents the resistance of charge transfer through the iron-deficient layer.  $R_p$  element is a measure of charge transfer in the pores of the product layer, which is described as Fe-Hydroxide/Oxide layer (Ertekin et al 2016; Pang and Chander 1990).  $C_{sl}$  corresponds to the capacitance of the surface layer, which indicates the formation of surface layer such as the initial pyrite oxidation species or the adsorbed collector/depressant species (Guo et al, 2016). The double-layer capacitance ( $Q_{dl}$ ) is represented in terms of a constant phase element (CPE) that indicates a nonhomogeneous surface (Ekmekeçi et al, 2010). Besides,  $R_{ct}$  element is related to the electrochemical process in the product coating, which helps to explain the formation of collector or

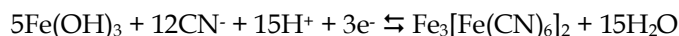
depressant layers. Such electrochemical processes may occur as charge transfer reactions, adsorption, and desorption processes. The net rate of electrochemical reactions on electrode surfaces is inversely proportional to  $R_{ct}$  value (Mu et al, 2017). In order to compare the adsorption behaviour of the depressants and the collector quantitatively, the EIS spectrum of each experiment was fitted to the equivalent electrical circuit model. The calculated  $R_{ct}$  values were compared to explain the mineral behaviour in the absence and presence of depressants and collector.

### 3. Results and discussion

Understanding the surface chemistry of minerals is of great importance in order to explain flotation processes. Many factors such as pH, type of reagents, oxygen content, etc. can affect the reactions occurring on the mineral surface. In this study, the adsorption behaviour of three depressants (NaCN, SMBS, and Aero7261A) used mainly for pyrite depression was investigated by the EIS technique. NaCN is known as one of the most common depressants for pyrite in the flotation process (Zhao et al, 2016). Simply, cyanide compounds are dissolved in water according to the following reaction:



The most acceptable reaction for the poisoning of pyrite surface by cyanide has been found to be the formation of insoluble cyanoferrate complexes. Hexacyanide compounds are formed by the reduction of the ferric hydroxide layer that occurred on the pyrite surface in the presence of cyanide (Moslemi and Gharabaghi 2017; Kocabag and Güler 2007):



Depression of pyrite by SMBS is more complicated compared to cyanide. The formation of a metal sulfite layer can inhibit the adsorption of the collector on the pyrite surface (Mu et al 2016b). It has also been reported that sulfite ions promote the formation of iron/copper hydroxides on the pyrite surface due to oxygen consumption causing the surface to become hydrophilic (Mu et al, 2016a).

Aero7261A is a modified polyacrylamide based water-soluble polymer used for the depression of iron sulphide minerals. The chemistry and interaction of this polymeric compound upon the heterogeneous mineral surface adsorption are highly complex due to the presence of various functional groups. Generally, the polymer is thought to adsorb onto the mineral surface via various interactions such as electrostatic, hydrogen bonding, chemical, and/or hydrophobic interactions (Mu et al, 2016a, Boulton et al 2001).

In this study, EIS experiments were performed in an alkaline solution (pH 9.2), where the pyrite can be depressed by the use of cyanide, SMBS and polyacrylamide-based depressants. Moderately alkaline pulp conditions are generally preferred over strongly alkaline conditions (>pH 11.5) for pyrite depression to minimize lime consumption and scaling problems in flotation circuits (Guo et al 2016). Effects of the sequence of addition of collector and depressant were also investigated.

#### 3.1. Results of EIS measurements on Sample A

Fig. 3 shows Bode and Nyquist plots of Sample A obtained in the presence and absence of the depressants and the collector. The electrical equivalent circuit model parameters were derived by fitting the experimental data using Gamry Echem Analyst software. The impedance parameters obtained for Sample A electrode in the presence of collector and depressants are summarized in Table 2. The fitting curves are shown as solid lines in the Nyquist plots. The fitting error (Chi-squared) to the proposed equivalent electrical circuit was very small ( $<1 \times 10^{-3}$ ) for all experiments (Table 2).

$R_{ct}$  represents the resistance of charge transfer through the iron-deficient layer, which changes according to the reaction between iron and depressants. The  $R_{ct}$  is inversely proportional with the surface reactivity. A lower  $R_{ct}$  value indicates a higher current flow for the electrochemical reactions on the pyrite surface (Mu et al, 2013). In other words, pyrite has high surface reactivity when the  $R_{ct}$  value is low.

Adsorption of xanthate on sulfide minerals leads to a decrease in capacitance due to its low dielectric constants (Guo et al, 2016; Venter and Vermaak, 2018). The capacitance is inversely proportional with surface resistance, but the adsorption of xanthate does not necessarily increase the  $R_{ct}$ . Addition of xanthate can decrease both the capacitance and  $R_{ct}$  due to the removal of oxidation products from the

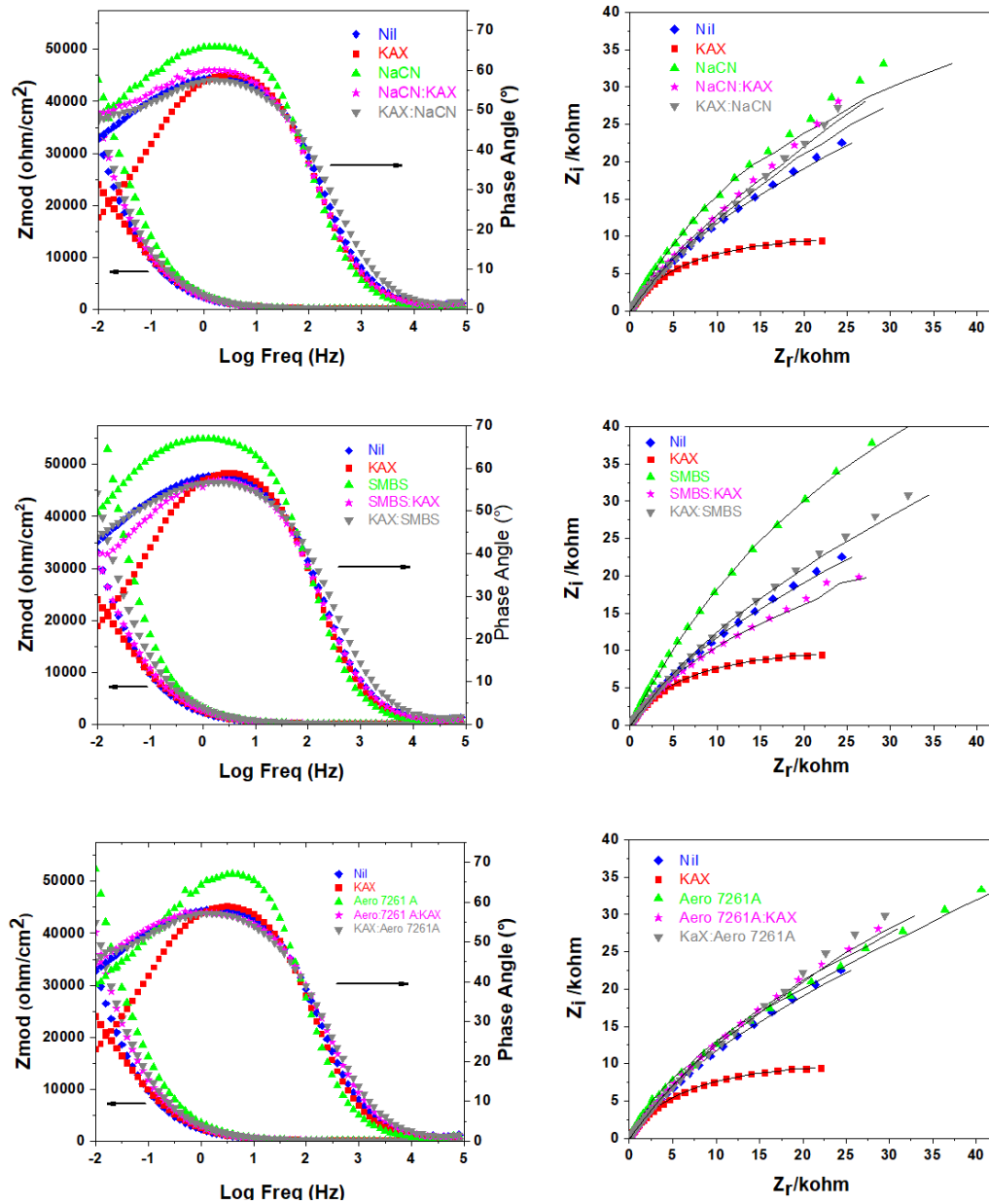


Fig. 3. EIS results of Sample A obtained in the presence and absence of different types of depressants upon KAX at pH 9.2 and 100 mV polarization potential (Experimental (scattered line) and fitted (solid line) for Nyquist plot)

Table 2. Parameters of the equivalent circuit simulated from EIS data for Sample A

Sample A	$R_s$ ( $\Omega^*cm^2$ )	$C_{s1}$ ( $F^*cm^{-2}$ )	$R_p$ ( $\Omega^*cm^2$ )	$Y_o$ ( $Ss^n cm^{-2}$ )	$n$	$R_{ct}$ ( $\Omega^*cm^2$ )	Chi-squared $\chi^2$
Nil	27.84	$2.50 \times 10^{-5}$	$1.20 \times 10^1$	$3.23 \times 10^{-4}$	0.62	$3.94 \times 10^4$	$1.86 \times 10^{-4}$
KAX	31.30	$2.64 \times 10^{-5}$	$1.41 \times 10^1$	$2.62 \times 10^{-4}$	0.64	$1.21 \times 10^4$	$3.68 \times 10^{-4}$
NaCN	30.83	$4.64 \times 10^{-5}$	$2.58 \times 10^1$	$2.26 \times 10^{-4}$	0.61	$1.43 \times 10^5$	$2.75 \times 10^{-3}$
NaCN:KAX	29.87	$2.79 \times 10^{-5}$	$1.29 \times 10^1$	$3.10 \times 10^{-4}$	0.63	$6.20 \times 10^4$	$6.13 \times 10^{-4}$
KAX:NACN	29.92	$1.43 \times 10^{-6}$	$1.09 \times 10^1$	$2.85 \times 10^{-4}$	0.61	$6.08 \times 10^4$	$1.04 \times 10^{-3}$
SMBS	32.84	$3.79 \times 10^{-5}$	$3.49 \times 10^1$	$1.76 \times 10^{-4}$	0.68	$9.28 \times 10^4$	$5.92 \times 10^{-4}$
SMBS:KAX	34.40	$2.01 \times 10^{-5}$	$1.32 \times 10^1$	$2.85 \times 10^{-4}$	0.62	$2.84 \times 10^4$	$3.69 \times 10^{-4}$
KAX:SMBS	34.44	$1.12 \times 10^{-5}$	$1.17 \times 10^1$	$2.42 \times 10^{-4}$	0.62	$5.93 \times 10^4$	$2.86 \times 10^{-4}$
7261 A	35.87	$4.28 \times 10^{-5}$	$2.39 \times 10^1$	$1.68 \times 10^{-4}$	0.60	$4.72 \times 10^4$	$7.59 \times 10^{-4}$
7261 A: KAX	33.11	$1.65 \times 10^{-5}$	$1.54 \times 10^1$	$2.72 \times 10^{-4}$	0.62	$5.66 \times 10^4$	$2.74 \times 10^{-4}$
KAX:7261 A	34.95	$1.25 \times 10^{-5}$	$1.38 \times 10^1$	$2.55 \times 10^{-4}$	0.62	$5.77 \times 10^4$	$6.09 \times 10^{-4}$

surface (Ertekin et al, 2016). However, the depressants affect directly the surface resistance ( $R_{ct}$ ) through the formation of stable and hydrophilic species at the surface. Therefore,  $R_{ct}$  was taken as a proxy for evaluation effects of various depressants in the presence and absence of xanthate.

As shown in Table 2, the interaction between Sample A and KAX has the lowest  $R_{ct}$ , which indicates a higher rate of adsorption of the collector. The addition of NaCN and hence the formation of cyanoferrate complex on the surface of pyrite increased  $R_{ct}$ , indicating surface coverage by a stable and electrochemically passive hydrophilic layer.  $R_{ct}$  values were lower in the presence of polymer-based depressant (Aero7261A) than the other depressants.

The adsorption process is coupled with the charge transfer in the pyrite-collector/depressant system because it is generally agreed that the composition and structure of the surface products depend on the redox potential (Guo, 2016). Therefore, the adsorption behaviour of the depressants used in this study was evaluated based on coating layer resistance ( $R_{ct}$ ) values. The  $R_{ct}$  is inversely proportional to the net rate of the reactions in the coating layer on electrode surfaces (Mu et al, 2017). Fig. 4 shows the  $R_{ct}$  values estimated for Sample A under different experimental conditions. The notation "Nil" represents the measurements in the absence of collector and depressants. "KAX" corresponds to the measurements in the presence of collector potassium amyl xanthate. Influence of depressant addition and sequence of addition of the depressants and the collector is also illustrated in the same graph. It must be noted that the comparison between the different experimental conditions should be done in reference to their base condition, i.e. "KAX" and "Dep" should be compared to "Nil"; "Dep:KAX" to "Dep"; "KAX:Dep" to "KAX" as base conditions.

Fig. 4 shows that the addition of NaCN increased the coating resistance considerably. This means that the adsorption of NaCN, presumably in the form of  $(Fe_4(Fe(CN)_6)_3)$ , caused the formation of a highly electrochemically resistive layer. Similar experiments were performed in the presence of SMBS and 7261A as pyrite depressants. These depressants also increased  $R_{ct}$  but at lower levels than that of NaCN. The depressing strength of the three depressants was in the order of NaCN>SMBS>7261A according to the  $R_{ct}$  values. These results are in agreement with the literature investigating the effects of these depressants on the flotation of pyrite in sulfide ores (Moslemi and Gharabaghi, 2017; Mu et al, 2016a; Zhao et al, 2016; Boulton et al, 2001; Zhu et al, 2013).

Effects of the sequence of addition of NaCN and KAX were also investigated. The  $R_{ct}$  values of "Dep:KAX" were compared to "Dep" as the base condition. Addition of KAX after conditioning with NaCN and SMBS decreased the  $R_{ct}$  values considerably, showing adsorption of collector even after conditioning with these strong depressants. This could be attributed to the low sulfur content but high Au and As contents of Sample A (Table 1). It is likely that there were spots on the pyrite surface where the collector molecules could adsorb. 7161A was the least effective depressant and increased slightly the  $R_{ct}$  value. The addition of KAX did not change the  $R_{ct}$  significantly, and it was similar to that of measured with NaCN:KAX.

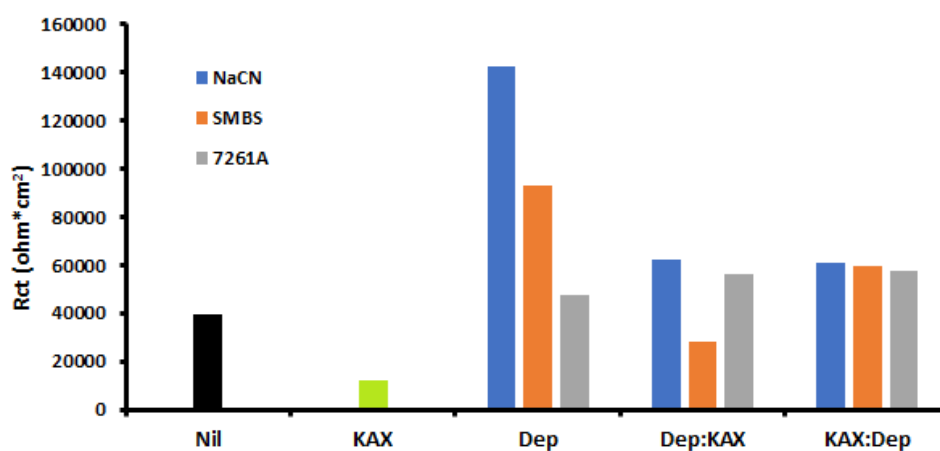


Fig. 4. Coating resistance ( $R_{ct}$ ) of Sample A under different experimental conditions at pH 9.2, 100 mV polarization potential. (Nil: absence of collector and depressants; KAX: collector; Dep:depressant; Dep:KAX depressant addition prior to KAX, and KAX:Dep KAX addition prior to depressant)

Effects of addition of depressant after conditioning with KAX were also investigated. The  $R_{ct}$  values of "KAX:Dep" were compared with "KAX" as the base condition. It is clear that addition of depressant removed some of the previously adsorbed collector molecules and produced  $R_{ct}$  values close to that of "Dep:KAX" condition. The results show that the sequence of addition of the depressants and the collector was not significant for Sample A, except SMBS.

### 3.2. Results of EIS measurements on Sample B

Similar experiments were performed using Sample B electrode. The chemical and electrochemical characteristics of Sample B were different from that of Sample A. Sample B was less electrochemically reactive. Therefore, differences in adsorption behaviour of the depressants and collector could be expected between the two pyrite samples.

Fig. 5 shows Bode and Nyquist plots of Sample B obtained in the presence and absence of the depressants and the collector. The fitted model parameters from the same equivalent circuit are given in Table 3. Adsorption behaviour of the depressants and collector was evaluated based on the calculated

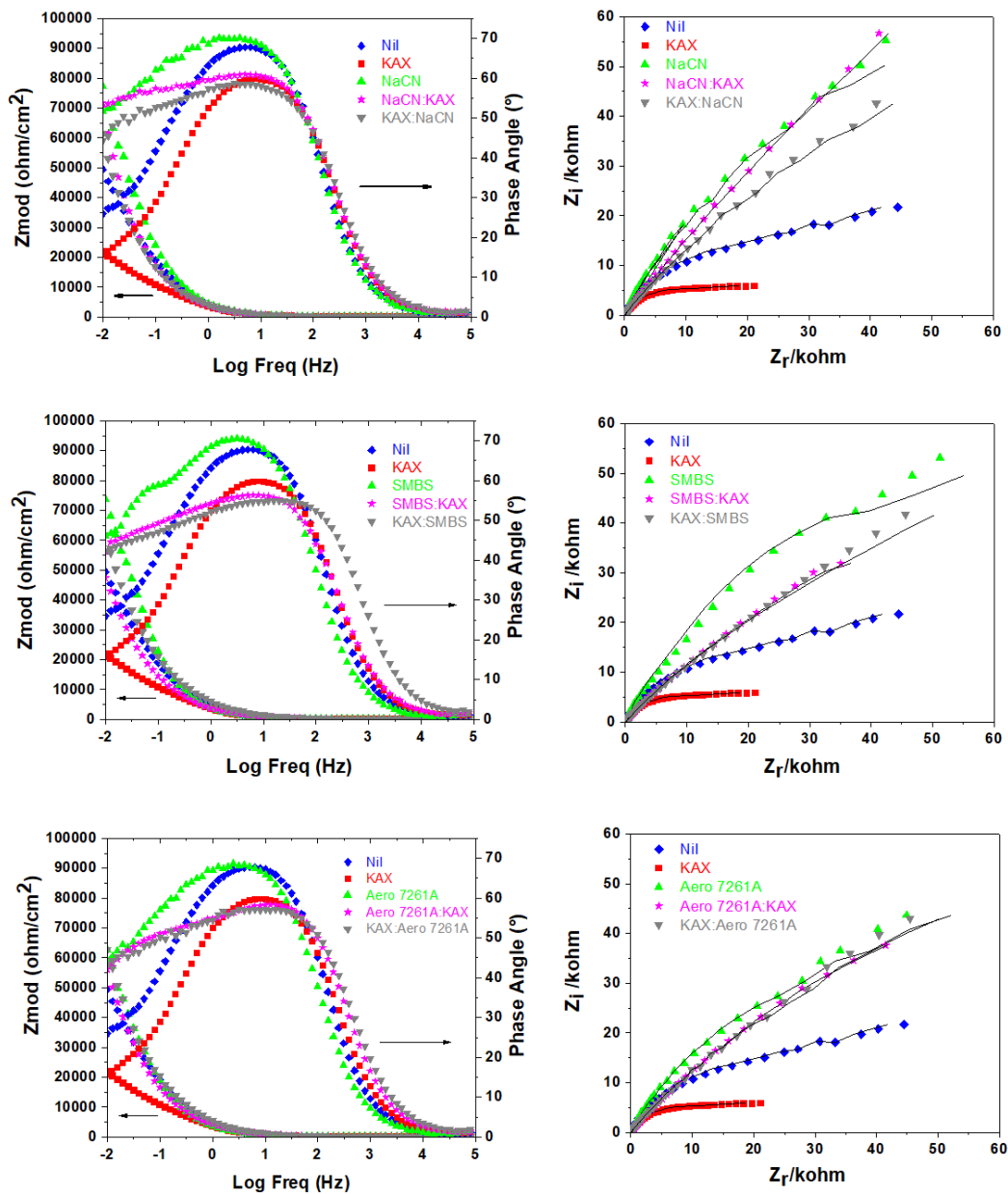


Fig. 5. EIS results of Sample B obtained in the presence and absence of different types of depressants at pH 9.2 and 100 mV polarization potential (Experimental (scattered line) and fitted (solid line) for Nyquist plot)

Table 3. Parameters of the equivalent circuit simulated from EIS data for Sample B

Sample B	$R_s$ ( $\Omega \cdot \text{cm}^2$ )	$C_{sl}$ ( $\text{F} \cdot \text{cm}^{-2}$ )	$R_p$ ( $\Omega \cdot \text{cm}^2$ )	$Y_o$ ( $\text{Ss}^n \cdot \text{cm}^{-2}$ )	$n$	$R_{ct}$ ( $\Omega \cdot \text{cm}^2$ )	Chi-squared $\chi^2$
Nil	32.72	$2.86 \times 10^{-5}$	$2.98 \times 10^1$	$1.14 \times 10^{-4}$	0.64	$2.58 \times 10^4$	$1.63 \times 10^{-3}$
KAX	32.07	$1.86 \times 10^{-5}$	$1.59 \times 10^1$	$1.66 \times 10^{-4}$	0.62	$9.72 \times 10^3$	$1.52 \times 10^{-3}$
NaCN	34.40	$3.05 \times 10^{-5}$	$4.04 \times 10^1$	$1.14 \times 10^{-4}$	0.63	$1.53 \times 10^5$	$2.95 \times 10^{-3}$
NaCN:KAX	33.91	$1.42 \times 10^{-5}$	$7.89 \times 10^0$	$1.64 \times 10^{-4}$	0.63	$1.55 \times 10^6$	$5.01 \times 10^{-4}$
KAX:NACN	37.83	$1.20 \times 10^{-5}$	$1.20 \times 10^1$	$1.68 \times 10^{-4}$	0.60	$1.20 \times 10^5$	$2.42 \times 10^{-4}$
SMBS	36.93	$3.95 \times 10^{-5}$	$4.25 \times 10^1$	$1.11 \times 10^{-4}$	0.66	$8.21 \times 10^4$	$1.86 \times 10^{-3}$
SMBS:KAX	41.28	$1.24 \times 10^{-5}$	$9.98 \times 10^0$	$1.92 \times 10^{-4}$	0.57	$8.77 \times 10^4$	$2.04 \times 10^{-4}$
KAX:SMBS	37.80	$5.42 \times 10^{-6}$	$8.80 \times 10^0$	$1.35 \times 10^{-4}$	0.55	$1.17 \times 10^5$	$6.37 \times 10^{-4}$
7261 A	38.01	$3.56 \times 10^{-5}$	$3.29 \times 10^1$	$1.36 \times 10^{-4}$	0.64	$7.10 \times 10^4$	$1.03 \times 10^{-3}$
7261 A: KAX	33.73	$1.15 \times 10^{-5}$	$6.72 \times 10^0$	$1.70 \times 10^{-4}$	0.58	$1.05 \times 10^5$	$8.82 \times 10^{-5}$
KAX:7261 A	38.88	$8.19 \times 10^{-6}$	$1.26 \times 10^1$	$1.40 \times 10^{-4}$	0.58	$1.09 \times 10^5$	$6.32 \times 10^{-4}$

$R_{ct}$  values (Fig. 6). The impedance value in the low-frequency region of Bode plots was significantly higher as a result of cyanide addition, which increased the value of  $R_{ct}$  (Table 3). Addition of NaCN increased the coating resistance drastically and inhibited adsorption of KAX on Sample B. NaCN was the strongest depressant tested for Sample B according to the  $R_{ct}$  values.

It is clear that the addition of NaCN prior to KAX (NaCN:KAX) inhibited almost completely the collector adsorption. Prestidge et al. has also reported that cyanide can significantly depress pyrite when it is added prior to the addition of collectors (Prestidge et al, 1993). A similar response was observed in the presence of SMBS and 7261A.  $R_{ct}$  values were slightly higher in "Dep:KAX" experiments compared to that of "Dep" experiments. The addition of KAX did not significantly affect the adsorption of the depressants for Sample B. However, the response of Sample B was different to that of Sample A in the presence of depressants. This difference is discussed in the next section of the paper.

When the depressants were introduced after KAX, the reactions occurred in favour of the depressant adsorption. Comparison of the  $R_{ct}$  values of KAX and "KAX:Dep" experiments showed that the depressants could replace the previously adsorbed KAX molecules and create a hydrophilic surface. This could be due to the competition for adsorption between the collector and depressant molecules, and the depressant molecules formed more stable compounds at the surface of pyrite particles.

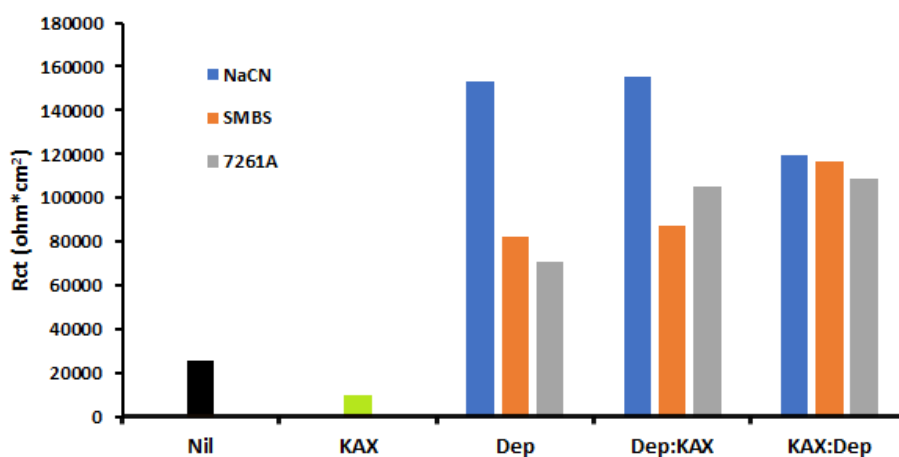


Fig. 6. Coating resistance ( $R_{ct}$ ) of Sample B under different experimental conditions at pH 9.2, 100 mV polarization potential. (Nil: absence of collector and depressants; KAX: collector; Dep:depressant; Dep:KAX depressant addition prior to KAX and KAX:Dep KAX addition prior to depressant)

### 3.3. The relationship between mineral composition and adsorption of depressants

The pyrite in Sample A contains higher As (in the form of Arsenopyrite) and Au, but lower S than that of Sample B. The presence of arsenopyrite in Sample A was considered as the main reason for the

differences in electrochemical characteristics and adsorption behaviour between the two samples. Sample A was more electrochemically active than Sample B according to the EIS spectra given in Fig. 3 and Fig. 5, respectively. The chemical composition and electrochemical classification of the pyrite samples line up with the EIS results. Given that these two pyrite samples act completely different in the presence of depressants.

As it was described in the previous above, the response of the electrodes to adsorption of the collector and depressants was evaluated based on the differences in  $R_{ct}$  values. For example, the difference in  $R_{ct}$  of “Nil” and “KAX” gives information about the adsorption of the collector, the difference between “Nil” and “Dep” shows adsorption of the depressants, etc.

Fig. 7 shows the differences in  $R_{ct}$  values to evaluate adsorption of KAX and the depressants (NaCN, SMBS and 7261A) on the pyrite surface in Sample A and Sample B.  $\Delta R_{ct}$  of KAX was negative for both samples indicating adsorption of xanthate molecules. A higher rate of adsorption was observed with Sample A, which could be attributed to its higher electrochemical activity and Au content (Ertekin et al, 2016). It has been shown that Au-containing pyrite particles have better collector adsorption and flotation performance than that of barren pyrite (Dunne, 2005; Huai et al, 2017; Monte et al, 1997; Huai et al 2019; Klimpel, 1999).

NaCN was the strongest depressant, and  $\Delta R_{ct}$  of NaCN was considerably higher than the other depressants. The rate of adsorption of SMBS and 7261A on the pyrite samples was similar.  $\Delta R_{ct}$  values of Sample B were slightly higher, particularly for NaCN and 7261A, indicating a higher rate of adsorption compared to Sample A.

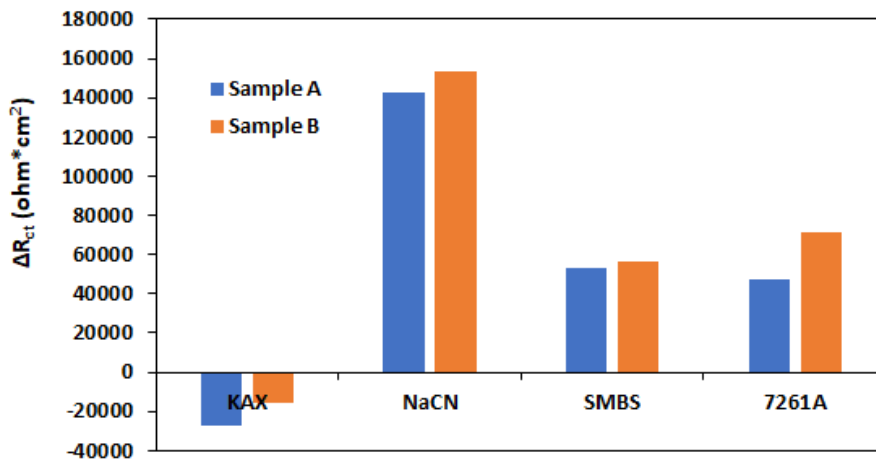


Fig. 7. The differences in  $R_{ct}$  values of “Nil” and the experiments conducted with KAX, NaCN, SMBS and 7261A

Adsorption of KAX on pyrite conditioned with the depressants was evaluated based on the differences between “Dep” and the experiments performed with depressants and collector (NaCN:KAX, SMBS:KAX, 7261A:KAX). Fig. 8 shows that  $\Delta R_{ct}$  values of NaCN and SMBS of Sample A were negative after collector addition. This means that the collector molecules adsorbed on the surface even after conditioning with the strong depressants. It is likely that there were spots, such as Au containing sites, on the surface of pyrite suitable for collector adsorption. This was not observed with 7261A, because it is a polysaccharide-based depressant, which adsorbs in the form of colloidal precipitates.

Sample B showed completely different adsorption behaviour.  $\Delta R_{ct}$  was positive for all depressants, which means that the collector molecules could not adsorb on the surface after conditioning with the depressants. Effects of the sequence of collector and depressant addition are shown in Fig. 9. In these experiments, the electrodes were conditioned with KAX first and then with the depressants. Therefore, the  $R_{ct}$  values were compared to the experiment performed with collector only “KAX”.  $\Delta R_{ct}$  values were positive for both samples, indicating adsorption of depressants after conditioning with the collector.  $\Delta R_{ct}$  values of Sample B were considerably higher than that of Sample A. That means the pyrite in Sample B can effectively be depressed even after conditioning with KAX, a long chain and strong collector, compared to Sample A.

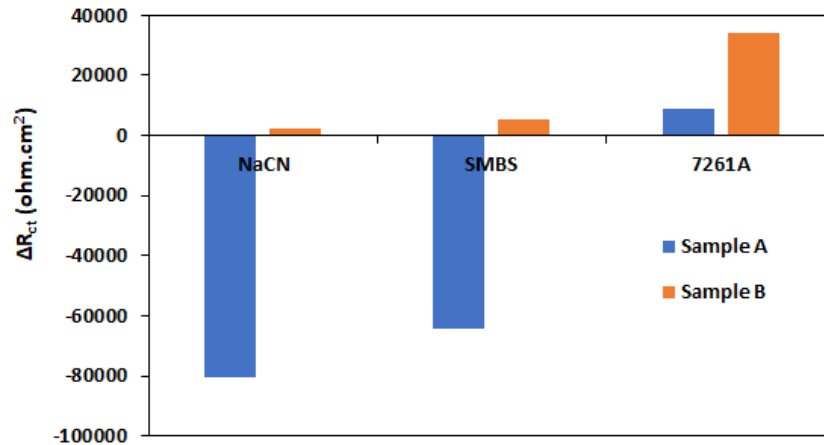


Fig. 8. The differences in  $R_{ct}$  values of "Dep" and the experiments conducted with NaCN:KAX, SMBS:KAX and 7261A:KAX

Sample B can be considered as a pure pyrite sample with minor defects and responds to the addition of depressants as demonstrated by a number of researches and industrial applications. Sample A, on the other hand, contains a significant amount of Au and As, which significantly affect the electrochemical characteristics of the pyrite and hence the response to the depressants in this case.

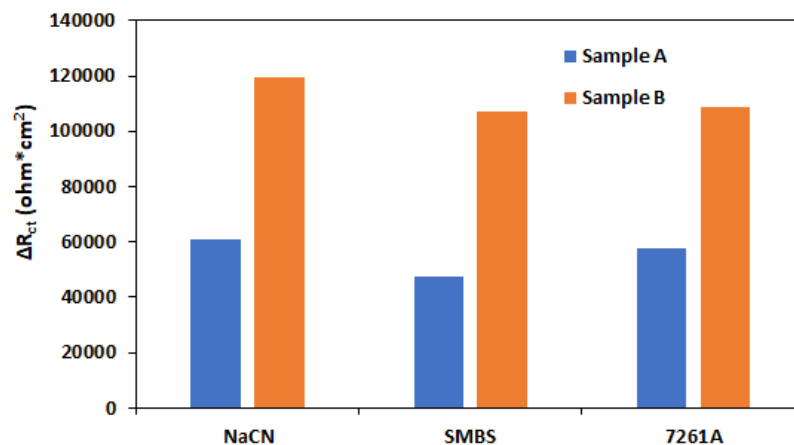


Fig. 9. The differences in  $R_{ct}$  values of "KAX" and the experiments conducted with KAX:NaCN, KAX:SMBS and KAX:7261A

#### 4. Conclusions

In this study, adsorption of three different depressants (NaCN, SMBS, and Aero7261A) on a Carlin trend ore (Sample A) and a sulfidic ore from South America (Sample B) was investigated by EIS measurement. The Chemical and hence electrochemical properties of the two pyrite samples were different. Sample A was more electrochemically active than Sample B according to the EIS spectra. Therefore, the rate of adsorption of the collector and the depressants was different for the two samples. A higher rate of collector adsorption was observed with Sample A. Besides, Sample B showed a higher affinity towards adsorption of depressants than that of Sample A.

According to EIS results, NaCN was the most effective depressant for both types of pyrite samples, followed by SMBS and 7261A. The sequence of addition of collector (KAX) and depressant was also discussed in detail for both samples. As a result, the sequence of addition of the collector and depressants was significant for Sample A. Adsorption of the collector was observed after conditioning with the depressants. This was attributed to the presence of Au containing sites at the surface, which are suitable for collector adsorption even after the use of strong pyrite depressants such as NaCN. On the other hand, Sample B showed a completely different response to the sequence of addition of collector and depressants. The collector molecules could not adsorb on the pyrite particles conditioned with the

depressants. When the samples were conditioned first with the collector and then with the depressants, adsorption of depressants was observed for both samples, but at different rates.  $\Delta R_{ct}$  values of Sample B were considerably higher than that of Sample A.

It can be concluded that EIS measurement is a useful method for testing various types of reagents for flotation conditions. EIS can be used as an alternative technique to the conventional batch scale flotation tests for pre-screening of various flotation reagents. Further tests should be conducted to link the EIS results, e.g.  $R_{ct}$  values to flotation performance, grade, recovery, selectivity, etc.

### Acknowledgements

The authors gratefully acknowledge the financial support of this research by Newmont Corporation.

### References

- ABRAMOV A.A., AVDOHIN V.M., 1997. *Oxidation of Sulfide Minerals in Beneficiation Processes*, Gordon and Breach Science Publishers, 319.
- ACKERMAN P., HARRIS G., KLIMPEL R., APLAN F., 1987. *Evaluation of flotation collectors for copper sulfides and pyrite, III. Effect of xanthate chain length and branching*, International journal of mineral processing, 21, 141-156.
- AI G., HUANG W., YANG X., LI X., 2017. *Effect of collector and depressant on monomineralic surfaces in fine wolframite flotation system*, Separation and Purification Technology, 176, 59-65.
- ALLISON S.A., GOLD L.A., NICOLE M.J., GRANVILLE A., 1972. *A determination of the products of reaction between various sulphide minerals and aqueous xanthate solution, and a correlation of the products with electrode rest potentials*, Metal. Trans, 3, 2613-2618.
- BICAK O., EKMEKCI Z., BRADSHAW D., HARRIS P., 2007. *Adsorption of guar gum and CMC on pyrite*, Minerals engineering, 20, 996-1002.
- BOULTON A., FORNASIERO D., RALSTON J., 2001. *Selective depression of pyrite with polyacrylamide polymers*, International Journal of Mineral Processing, 61 (2001) 13-22.
- CHANDRA A., GERSON A.R., 2010. *The mechanisms of pyrite oxidation and leaching: a fundamental perspective*, Surface Science Reports, 65, 293-315.
- DUNNE R., 2005. *Flotation of gold and gold-bearing ores*, Developments in mineral processing, 15, 309-344.
- EKMEKCI Z., ASLAN A., HASOY H., 2004. *Effects of EDTA on Selective Flotation of Sulphide Minerals*, Physicochemical Problems of Mineral Processing, 38, 9-94.
- EKMEKCI Z., BAGCI E.T., CAN M., BICAK Ö., PEKMEZ K., 2016. *Electrochemical predictions of flotability. The Optimization of Mineral Processes by Modelling and Simulation 2008-2011*, AMIRA P90 Mineral Processing, 417-486.
- EKMEKCI Z., BECKER M. B., BAGCI E. T., BRADSHAW D., 2010. *An impedance study of the adsorption of CuSO<sub>4</sub> and SIBX on pyrrhotite samples of different provenances*, Minerals Engineering, 23, 903-907.
- EKMEKCI Z., BECKER M., TEKES E.B., BRADSHAW D., 2010. *The relationship between the electrochemical, mineralogical and flotation characteristics of pyrrhotite samples from different Ni Ores*, Journal of Electroanalytical Chemistry, 647, 133-143.
- ERTEKIN Z., PEKMEZ K., EKMEKCI Z., 2016. *Evaluation of collector adsorption by electrochemical impedance spectroscopy*, International Journal of Mineral Processing, 154, 16-23.
- FORBES E. F., SMITH L., VEPSALAINEN M., 2018. *Effect of pyrite type on the electrochemistry of chalcopyrite/pyrite interactions*, Physicochem. Probl. Miner. Process. 54 (4), 1116-1129.
- GOOLD L.A., FINKELSTEIN N.P., 1972. *The reaction of sulphide minerals with thiol compounds*. NIMM, Johannesburg, South Africa, Report No, 1439.
- GUO B., 2016. *The Poisoning of Pyrite Surface upon Xanthate Adsorption by Cyanide in Mildly Acidic Media*, Electroanalysis, 28, 724-732.
- GUO B., LIN X., FU W., KU J., 2020. *Establishment of electrochemical methods to examine the adsorption of flotation surfactants onto a mineral surface*, Journal of Chemical Technology & Biotechnology, 95, 1580-1589.
- GUO B., PENG Y., PARKER G., 2016. *Electrochemical and spectroscopic studies of pyrite-cyanide interactions in relation to the depression of pyrite flotation*, Minerals Engineering, 92, 78-85.
- HUAI Y., PLACKOWSKI C., PENG Y., 2017. *The surface properties of pyrite coupled with gold in the presence of oxygen*, Minerals Engineering, 111, 131-139.

- HUAI Y., PLACKOWSKI C., PENG Y., 2019. *The effect of gold coupling on the surface properties of pyrite in the presence of ferric ions*, Applied Surface Science, 488, 277-283.
- HUANG Z., WANG J., SUN W., HU Y., CAO J., GAO Z., 2019. *Selective flotation of chalcopyrite from pyrite using diphosphonic acid as collector*, Minerals Engineering, 140, 105890.
- JIANG C., WANG X., PAREKH B., LEONARD J., 1988. *The surface and solution chemistry of pyrite flotation with xanthate in the presence of iron ions*, Colloids and Surfaces A: Physicochemical and Engineering Aspects, 136 51-62.
- KAPPES R., BROSNAHAN D., GATHJE J., 2010. *The effect of mineral liberation on the floatabilities of pyrite, arsenopyrite and arsenian pyrite for Carlin Trend ores*, Proceedings XXV international mineral processing congress, 2913-2926.
- KAPPES R., GATHJE J., 2010. *The metallurgical development of an enargite-bearing deposit*, Proceedings of the XXV International Mineral Processing Congress (IMPC), Brisbane, Australia, 6-10.
- KARIUKI J.K., 2012. *An electrochemical and spectroscopic characterization of pencil graphite electrodes*, Journal of the Electrochemical Society, 159, H747.
- KLIMPEL R., 1999. *Industrial experiences in the evaluation of various flotation reagent schemes for the recovery of gold*, Mining, Metallurgy & Exploration, 16, 1-11.
- KNOLL F., TAYLOR J., 1985. *Advances in electrostatic separation*, Mining, Metallurgy & Exploration, 2, 106-114.
- KOCABAG D., GULER T., 2007. *Two-liquid flotation of sulphides: An electrochemical approach*, Minerals Engineering, 20, 1246-1254.
- LAI C.-H., LU M.-Y., CHEN L.-J., 2012. *Metal sulfide nanostructures: synthesis, properties and applications in energy conversion and storage*, Journal of Materials Chemistry, 22, 19-30.
- LI L., POLANCO C., GHAREMAN A., 2016. *Fe (III)/Fe (II) reduction-oxidation mechanism and kinetics studies on pyrite surfaces*, Journal of Electroanalytical Chemistry, 774, 66-75.
- LI M., WEI D., LIU Q., LIU W., ZHENG J., SUN H., 2015. *Flotation separation of copper-molybdenum sulfides using chitosan as a selective depressant*, Minerals Engineering, 83, 217-222.
- MONTE M., LINS F., OLIVEIRA J., 1997. *Selective flotation of gold from pyrite under oxidizing conditions*, International journal of mineral processing, 51, 255-267.
- MONTEIRO M.C., KOPER M.T., 2019. *Alumina contamination through polishing and its effect on hydrogen evolution on gold electrodes*, Electrochimica Acta, 325, 134915.
- MOSLEMI H., GHARABAGHI M., 2017. *A review on electrochemical behavior of pyrite in the froth flotation process*, Journal of Industrial and Engineering Chemistry, 47, 1-18.
- MU Y., CHENG Y., PENG Y., 2020. *The interaction between grinding media and collector in pyrite flotation at neutral and slightly acidic pH*, Minerals Engineering, 145, 106063.
- MU Y., LI L., PENG Y., 2017. *Surface properties of fractured and polished pyrite in relation to flotation*, Minerals Engineering, 101, 10-19.
- MU Y., PENG Y., LAUTEN R.A., 2015. *Electrochemistry aspects of pyrite in the presence of potassium amyl xanthate and a lignosulfonate-based biopolymer depressant*, Electrochimica Acta, 174, 133-142.
- MU Y., PENG Y., LAUTEN R.A., 2016a. *The depression of pyrite in selective flotation by different reagent systems—A Literature review*, Minerals Engineering, 96, 143-156.
- MU Y., PENG Y., LAUTEN R.A., 2016b. *The mechanism of pyrite depression at acidic pH by lignosulfonate-based biopolymers with different molecular compositions*, Minerals Engineering, 92, 37-46.
- NICOL M.J., 2017. *The use of impedance measurements in the electrochemistry of the dissolution of sulfide minerals*, Hydrometallurgy, 169, 99-102.
- PANG J., CHANDER S., 1990. *Oxidation and wetting behavior of chalcopyrite in the absence and presence of xanthates*, Mining, Metallurgy & Exploration, 7, 149-155.
- PAUPORTE T., SCHUHMAN D., 1996. *An electrochemical study of natural enargite under conditions relating to those used in flotation of sulphide minerals*, Colloids and Surfaces A: Physicochemical and Engineering Aspects, 111, 1-19.
- PRESTIDGE C.A., RALSTON J., SMART R.S.C., 1993. *The competitive adsorption of cyanide and ethyl xanthate on pyrite and pyrrhotite surfaces*, International journal of mineral processing, 38, 205-233.
- RATH R., SUBRAMANIAN S., PRADEEP T., 2000. *Surface chemical studies on pyrite in the presence of polysaccharide-based flotation depressants*, Journal of Colloid and Interface Science, 229, 82-91.
- VALDIVIESO A.L., CERVANTES T.C., SONG S., CABRERA A.R., LASKOWSKI J., 2004. *Dextrin as a non-toxic depressant for pyrite in flotation with xanthates as collector*, Minerals engineering, 17, 1001-1006.

- VELASQUEZ P., LEINEN D., PASCUAL J., RAMOS-BARRADO J.R., GREZ P., GOMEZ H., SCHREBLER R., DEL RIO R., CORDOVA R. Cordova, 2005. *A chemical, morphological, and electrochemical (XPS, SEM/EDX, CV, and EIS) analysis of electrochemically modified electrode surfaces of natural chalcopyrite (CuFeS<sub>2</sub>) and pyrite (FeS<sub>2</sub>) in alkaline solutions*, *The Journal of Physical Chemistry B*, 109, 4977-4988.
- VENTER J.A., VERMAAK M.K.G., 2008. *EIS measurements of dithiocarbonate and trithiocarbonate interactions with pyrite and copper*, *Minerals Engineering* 21, 559-567.
- ZHANG W., SUN W., HU Y. Hu, CAO J., GAO Z., 2019. *Selective flotation of pyrite from galena using chitosan with different molecular weights*, *Minerals*, 9, 549.
- ZHAO C., HUANG D., CHEN J., LI Y., CHEN Y., LI W., 2016. *The interaction of cyanide with pyrite, marcasite and pyrrhotite*, *Minerals Engineering*, 95, 131-137.
- ZHAO S., GUO B., PENG Y., MAI Y., 2017. *An impedance spectroscopy study on the mitigation of clay slime coatings on chalcocite by electrolytes*, *Minerals Engineering*, 101, 40-46.
- ZHENG X.-F., LIU L.-Z., NIE Z.-Y., YANG Y., CHEN J.-H., YANG H.-Y., XIA J.-I., 2019. *The differential adsorption mechanism of hexahydrated iron and hydroxyl irons on a pyrite (1 0 0) surface: A DFT study and XPS characterization*, *Minerals Engineering*, 138, 215-225.
- ZHU Y.M., JIA J.W., MA Y.W., GAO P., HAN Y.X., ZHAO J.J., LI J.B., 2013. *Adsorption of Sodium Cyanide on Pyrite Particle Surface*, *Advanced Materials Research, Trans Tech Publ*, 3-9.